Published online 24 April 2021

Nucleic Acids Research, 2021, Vol. 49, No. 12 ***e71***
https://doi.org/10.1093/nar/gkab233

Efficient splicing-based RNA regulators for tetracycline-inducible gene expression in human cell culture and *C. elegans*

Monika Finke[1,2], Dominik Brecht[1], Julia Stifel[1,2], Karina Gense[2,3], Martin Gamerdinger[2,3] and Jörg S. Hartig[1,2,*]

[1]Department of Chemistry, University of Konstanz, Universitätsstraße 10, 78457 Konstanz, Germany, [2]Konstanz Research School Chemical Biology (KoRS-CB), University of Konstanz, Universitätsstraße 10, 78457 Konstanz, Germany and [3]Department of Biology, University of Konstanz, Universitätsstraße 10, 78457 Konstanz, Germany

Received February 08, 2021; Revised March 17, 2021; Editorial Decision March 21, 2021; Accepted April 23, 2021

ABSTRACT

Synthetic riboswitches gain increasing interest for controlling transgene expression in diverse applications ranging from synthetic biology, functional genomics, and pharmaceutical target validation to potential therapeutic approaches. However, existing systems often lack the pharmaceutically suited ligands and dynamic responses needed for advanced applications. Here we present a series of synthetic riboswitches for controlling gene expression through the regulation of alternative splicing. Placing the 5′-splice site into a stem structure of a tetracycline-sensing aptamer allows us to regulate the accessibility of the splice site. In the presence of tetracycline, an exon with a premature termination codon is skipped and gene expression can occur, whereas in its absence the exon is included into the coding sequence, repressing functional protein expression. We were able to identify RNA switches controlling protein expression in human cells with high dynamic ranges and different levels of protein expression. We present minimalistic versions of this system that circumvent the need to insert an additional exon. Further, we demonstrate the robustness of our approach by transferring the devices into the important research model organism *Caenorhabditis elegans*, where high levels of functional protein with very low background expression could be achieved.

INTRODUCTION

Synthetic devices that allow for conditional control of gene expression are indispensable for studying different aspects in cellular or organismal contexts. These synthetic switches are increasingly interesting for controlling gene expression in therapeutic applications, and even though a broad range of inducible systems is already available for work with prokaryotes, additional options for controlling gene expression in eukaryotic cells and organisms are in great demand. One popular choice used in various eukaryotic cell lines and organisms is the tetracycline-responsive Tet-ON/Tet-OFF system (1). The system is based on a transcription factor that originally controls expression of a tetracycline resistance operon in bacteria (1,2). Another example is the Q-repressible system, which is also based on transcriptional activators and repressors and has been introduced for gene regulation in multi-cellular organisms like *Caenorhabditis elegans* (3). However, such activator/repressor systems in eukaryotes rely on the expression of foreign transcription factors and leave a large genetic footprint within the engineered cell line or used model organism. A more elegant way to conditionally control gene expression has emerged with the development of artificial riboswitches. Found mostly in the 5′-UTR of bacterial mRNAs, riboswitches represent genetic control elements consisting solely of RNA. The high affinity and specific interaction of the RNA with its respective ligand leads to a change in gene expression on a transcriptional or translational level (4).

Like their natural counterparts, synthetic riboswitches are composed of two crucial domains: an aptamer domain that is responsible for binding the small effector molecule and an expression platform that provides the mechanism for modulating downstream gene expression. One bottleneck in creating artificial riboswitches, however, is the limited set of aptamers available to act as sensory domains. Although aptamers can be created *in vitro* against potentially any small-molecule ligand of choice via SELEX, not every aptamer that exhibits high affinity for its ligand undergoes sufficient conformational changes to be functional *in vivo* (5). On the other hand, if a well-suited aptamer is identified, it can often be used in many different setups in a very modular fashion. Suitable expression platforms range from roadblock mech-

*To whom correspondence should be addressed. Tel: +49 7531 88 4575; Email: joerg.hartig@uni-konstanz.de

anisms that interfere with ribosomal scanning and occlusion of miRNA target sites to the use of small self-cleaving ribozymes, which, when inserted into the untranslated regions of an mRNA, impact its stability (6–10). Optimized connection sequences between the two functional RNA domains need to be identified to couple the ligand-binding event in the aptamer domain with changes in the expression platform. Such communication modules can be optimized by rational design or via screening *in vitro* and *in vivo*, as well as through evolution experiments (11). The relatively few nucleotides constituting the communication module have often been shown to greatly impact the gene expression level and dynamic range of the designed switches. Assembled from these building blocks, synthetic riboswitches can be used as control devices in diverse cellular contexts. Although several different expression platforms have been described so far, such systems still often lack robustness, high switching performance, or inter-organismal transferability. In this study, we make use of the widespread mechanism of alternative splicing in eukaryotes in order to engineer efficient RNA switches. Alternative splicing greatly contributes to the diversity of the human proteome: >90% of all human genes are alternatively spliced (12). Controlling alternative splicing allows for the creation of different protein isoforms and thus yields the possibility of generating newly engineered proteins by inserting or skipping exons.

Aptamer-based splicing control has already been described by Süß and coworkers using the tetracycline aptamer. In one case, they obtained efficient inhibition of pre-mRNA splicing in yeast by inserting the aptamer close to the 5′-splice site (SS) with the consensus sequence of the SS located within the aptamer stem (13). A more rigid structure of the aptamer stem, upon ligand binding, led to an inaccessible SS and thus an altered mRNA. A very similar setup was later used in a design where the 3′-SS of the first intron was included in the stem of a tetracycline-binding aptamer (14). With this design it was possible to control exon skipping in mammalian cells in four different genetic contexts, demonstrating the robustness of this expression platform for synthetic riboswitches. However, although the concept in this study is very promising, an improvement of the dynamic range of these switches would be beneficial for a more widespread use of such systems in different applications.

As a starting point for developing novel efficient and robust RNA switches based on exon skipping, we adapted a design that has been introduced in a patent (15). A synthetic construct consisting of an intron-alternative exon-intron cassette was inserted into the coding frame of the firefly luciferase (*hluc*+) (Figure 1A). The alternative exon contains a premature termination codon (PTC) leading to a mutated mRNA version that becomes susceptible to nonsense-mediated decay (NMD). In the event, that it escaped the NMD pathway, the mRNA version would further result in a shortened nonfunctional protein (16,17). In order to control the incorporation of this exon via an external stimulus, the 5′-SS of the second intron was sequestered within the closing stem of an aptamer. Presence of the respective ligand determines the accessibility of the 5′-SS and thereby controls splicing of the mRNA. In the absence of the small molecule effector, the 5′-SS is accessible, and the insertion of the alternative exon leads to an altered mRNA containing the PTC. However, the effector ligands theophylline and guanine are not considered well-suited with regard to applications of such RNA switches in eukaryotic model organisms or for future therapeutic approaches in patients. Concerning toxicity and bioavailability, a more favorable aptamer-ligand pair represents the *in vitro* selected aptamer-binding tetracycline (18). Tetracycline shows very good bioavailability and is a marketed therapeutic with a toxicity profile that is also acceptable for certain therapeutic approaches (19,20). This allows for applications in various eukaryotic models like yeast, human cell culture, and *C. elegans* (1,13,21). The corresponding tetracycline-binding aptamer derived from SELEX experiments by Berens *et al.* is well characterized and shows high affinity and specificity for its ligand (18,22,23). Furthermore, it has been proven to be a suitable sensor domain for the development of artificial riboswitches in combination with different expression platforms (8,14,24,25).

Here, we present novel tetracycline-dependent RNA switches based on exon skipping. We exploited the tetracycline-binding aptamer to interfere with the accessibility of the 5′-SS. We investigated the influence of the location and the thermodynamic stability of the stem structure containing the splice site on the functionality of the RNA switches. The best-performing constructs resulting from this optimization show tight control of gene expression in HeLa cells. The developed RNA switches were then transferred to the multicellular model organism *C. elegans*, which until recently lacked efficient and convenient systems for the conditional control of gene expression (21). In our study, the designed switches even demonstrated superior performance and could be used to generate a new robust Huntington's disease model with a tetracycline inducible formation of insoluble polyQ protein aggregates. With very little to no background expression, this system greatly adds to the toolbox of genetic devices for the induction of gene expression in this widely used model organism. Taken together, we present artificial riboswitches that are triggered by a pharmaceutically suited small molecule that allows for potent control of transgene expression in human cell culture and *C. elegans*. Importantly, it functions without the need for additional regulatory proteins, permits the use of natural promotors, and requires very little coding space.

MATERIALS AND METHODS

Plasmid construction

Luciferase constructs. The psiCHECK™-2 vector (Promega) was used for luciferase reporter assays in HeLa cells. The vector carries a firefly luciferase *hluc*+ gene, and the *Renilla* luciferase *hRluc* gene serves as an internal control. The synthetic intron-alternative exon–intron construct designed by Boyne *et al.* was chemically synthesized (GeneArt) and inserted into the *hluc*+ gene using ApaI and XbaI restriction sites (15). Vector and insert were ligated using the Quick Ligation™ Kit (NEB) according to the manufacturer's protocol, resulting in the plasmid psiCHECK-splice (the sequence is shown in Supplementary Figure S1). Tetracycline aptamers were cloned downstream of the alternative exon via overhang extension PCR, resulting in the constructs Tet1_in-Tet9_ex, and

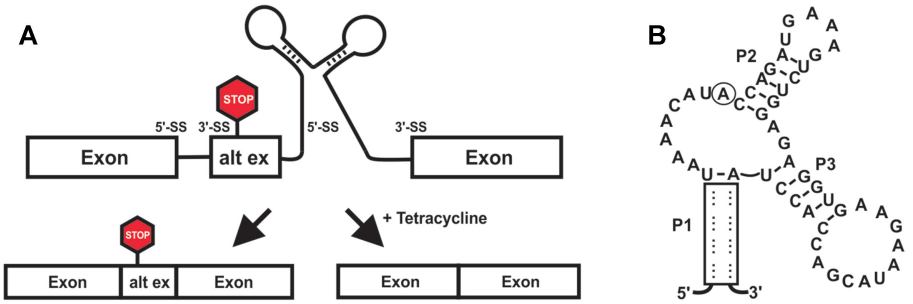

Figure 1. Schematic representation of the gene regulatory cassette and utilized aptamer sequence. (**A**) An alternative exon (alt ex) with an adjacent aptamer and flanking intron sequences is inserted into a split coding region of the gene of interest (boxed exons). The alternative exon carries a stop codon (red hexagon). In the absence of tetracycline, constitutive splicing incorporates the alternative exon into the mRNA. In the presence of tetracycline, exon skipping is triggered, leading to the exclusion of the alternative exon and expression of the functional full-length protein. (**B**) Sequence of the tetracycline-binding aptamer. Varying sequences of stem P1 are indicated by dotted lines. An A to U point mutation (circled) renders the aptamer binding deficient.

the following removal of the alternative exon was cloned via primer extension PCR, resulting in the constructs Tet10_el-Tet13_el (primer and construct sequences can be found in Supplementary Figure S2.)

mCherry constructs. The pCFJ910 plasmid with αNacp::mCherry::αNacUTR was kindly provided by the Deuerling lab (University of Konstanz) and was used for mCherry reporter assays. The alternative exon sequence with or without the subsequent tetracycline-binding aptamer as used in cell culture experiments was inserted 3′ of the first encoded intron using Gibson Assembly® with the primers 5′gtaactaaaggcggaccattac and 5′ctgaaaatttaaataatcagggttagttag for amplification of the vector and 5′ctgattatttaaattttcag and 5′aatggtccgcctttagttac for amplification of the respective insert. Ligation of the PCR fragments was carried out using the Gibson Assembly® Master Mix (NEB) following the manufacturer's instructions. In a second cloning step an additional intron (51nt in length) was inserted 3′ of the alternative exon-aptamer sequence using overhang extension PCR. (The sequence of the engineered mCherry can be found in Supplementary Figure S3.)

polyQ constructs. The inducible polyQ-Htt plasmids were constructed by exchanging mCherry with the Huntingtin exon 1 encoding sequences from plasmids p103QHtt.EGFP-N1 and p25QHtt.EGFP-N1 (kindly provided by the Deuerling Lab, University of Konstanz) using the Gibson Assembly® Master Mix (NEB) with the primers 5′tggacgaactatacaaatagcttgtttcctgatgaccttg and 5′agcttttccagggtcgccattgtttaatgtggtaaccc for amplification of the vector and the primers 5′atggcgaccctggaaaag and 5′ctatttgtatagttcgtccatgc for amplification of the inserts. The corresponding intron-alternative exon-intron cassette was subsequently cloned 27 nt downstream of the start codon of 103QHtt and 25QHtt, respectively, using the Gibson Assembly® Master Mix (NEB) with the primers 5′gccttcgagtccctcaaaag and 5′cttcatcagcttttccaggg for amplification of the vector and 5′ccctggaaaagctgatgaaggtaagtttaaacatatatatactaactaacc and 5′cttttgagggactcgaaggcctgaaaatttaaatatgtatggttagttag for amplification of the inserts.

Cell culture

Cell culture and cultivation. HeLa cells were cultivated in a medium consisting of Dulbecco's modified Eagle's medium (Gibco DMEM, Fisher Scientific) supplemented with 10% (v/v) fetal calf serum and 1 % (v/v) penicillin/streptomycin (Fisher Scientific) at 37°C and 5% CO_2 in a humidified atmosphere. The cells were passaged every 2–3 days, and no cells older than passage 40 were used.

Transient transfection. The day prior to transfection, the cells were seeded into 96-well plates at 15 000 cells/well. The cells were transfected using Lipofectamine® 3000 (Fisher Scientific) according to the manufacturer's instructions with 100 ng of respective plasmid DNA per well. After 4–6 h, the medium was exchanged with fresh medium with or without 50 μM tetracycline (Merck).

Dual luciferase reporter assay. After incubation of transiently transfected cells for 24 h with or without tetracycline, a dual luciferase assay was performed using the Dual-Luciferase® Reporter Assay System (Promega) according to the manufacturer's instructions. For luminescence measurement, a Spark® multimode microplate reader (Tecan) was used with a settle time of 0 ms and an integration time of 2000 ms. The ratio between the measured firefly and *Renilla* luminescence values was calculated for each well. Each experiment was performed in triplicate, and average values were set in correlation to the psiCHECK™-2 vector as 100%, which was measured on each plate. Propagation of errors was included in the given standard deviation.

RT-PCR analysis. On the day prior to transfection, cells were seeded into 12-well plates at 150 000 cells/well. The cells were transfected using Lipofectamine® 3000 (Fisher Scienctific) according to the manufacturer's instructions, with 100 ng of respective plasmid DNA per well. After 4–6 h, the medium was exchanged with fresh medium with or without 50 μM tetracycline (Merck). After incubating transiently transfected cells for 24 h with or without tetracycline, total RNA was isolated using the RNA isolation Quick-RNA™ Miniprep Kit (Zymo Research) according to the manufacturer's instruction. An additional DNaseI digest (Thermo Scientific™) with subsequent RNA purification (RNA Clean & Concentrator-100, Zymo Research)

was performed, and 500 ng of RNA was used for reverse transcription with random hexamers using the High Capacity cDNA Reverse Transcription Kit (applied Biosystems) following the accompanying protocol (10 min at 25°C, 120 min at 37°C, 5 min at 85°C). 1 μl of cDNA was used for subsequent PCR using Phusion HSII polymerase (New England Biolabs, initial denaturation 30 s at 98°C, 10 s at 98°C, 30 s 59°C, 20 s at 72°C, 30 cycles, final elongation 7 min at 72°C), and the product was analyzed on a 2% (w/v) agarose gel (primers are given in Supplementary Figure S2.)

qPCR analysis. qPCR analysis was performed using the GoTaq® qPCR Master Mix and the CFX Connect Real-Time PCR Detection System with 1 μl of cDNA as template (prepared as described for RT-PCR). Primers for firefly (*hluc*+) and *Renilla* (*hRluc*) luciferase were originally designed and validated by Beilstein *et al.* (10). (Primer sequences are given in Supplementary Figure S2.) For qPCR reactions, a 10 μl reaction volume was employed with final concentrations of 1× GoTaq® qPCR Master Mix, 250 nM primers and 1 μl cDNA. PCR conditions were initial denaturation at 95°C for 2 min followed by 40 cycles of 95°C for 15 s and 60°C for 60 s. To ensure qPCR specificity, a melt curve analysis followed showing single melting peaks, and qPCR amplicons were visualized as single bands of expected height on a 2% (w/v) agarose gel. Cq values were derived from analysis with Bio-Rad CFX Maestro 1.1 software. A no-template control was added to each plate, and each sample was measured in technical duplicates. Samples were further analyzed via the delta-Cq method with *hRluc* as a reference gene. Mean mRNA abundance was calculated from three independent experiments.

C. elegans culture

Cultivation and microinjection. In all experiments, *C. elegans* Bristol strain N2 was used for transformations. Worms were cultured on NGM agar plates according to standard techniques with *Escherichia coli* OP50 as the food source (26). Transgenic strains were generated using standard microinjection procedures (27). For each construct, at least two independent transgenic lines carrying extrachromosomal arrays were obtained and showed comparable results. In all transformations, the injection mixture comprised 2.5 ng/μl of the plasmid of interest, 10 ng/μl pPD152.79 (dpy-30p::GFP; gift from Andrew Fire, Addgene plasmid #1704) as co-injection marker and 90 ng/μl of GeneRuler 1 kb DNA Ladder (Fisher Scientific). All plasmids and the 1 kb DNA ladder were purified using the QIAprep Spin® Miniprep Kit (Qiagen). Stable transgenic lines were generated by X-ray mediated integration of extrachromosomal arrays (40 gy; X-RAD 225iX).

Tetracycline treatment. Tetracycline was dissolved in 100% ethanol (40 mM stock solution) and added to NGM plates in a final concentration of 10 μM before pouring. Semi-synchronized worms carrying the tetracycline-dependent reporters were grown on agar plates with or without 10 μM tetracycline for 3 days from hatch until adulthood at 20°C prior to assessment of mCherry and/or GFP expression using fluorescence microscopy and immunoblotting.

Fluorescence microscopy. For each strain, five transgenic worms were placed in a drop of 25 mM levamisole hydrochloride in M9-buffer on an empty NGM plate. Images were recorded using a Leica DM 5500B microscope using a 506505 10× objective and a DFC 365 FX CCD-Microscope Camera. The exposure time for the mCherry channel was adjusted to the control for animals that constitutively express mCherry and was then used for all constructs. Images were processed in Fiji (ImageJ) using cropping, brightness, and contrast tools (28). Contrast settings were adjusted for control animals that constitutively express mCherry and were then propagated to all other images.

Western blotting. For the detection of mCherry by western blotting, worms were grown on NGM agar plates with or without 10 μM tetracycline for 3 days from hatch until adulthood at 20°C. Worms were picked and placed in SDS-lysis buffer [62.5 mM Tris (pH 6.8), 1 mM EDTA (pH 8.0), 2 % (w/v) SDS, 10 % (w/v) sucrose] containing 1× protease inhibitor cocktail (Roche) and lysed by sonication. Samples were centrifuged and the supernatant was mixed with 5× SDS loading dye. Samples were applied to a 10 % SDS–bis–Tris gel (1.5 h, 100 V) in 1× MOPS running buffer and electroblotted onto a nitrocellulose membrane. The primary antibodies used in this study are anti-mCherry monoclonal mouse (Novus Biological, NBP1–96752) and anti-actin monoclonal mouse (Santa Cruz, sc-47778). Anti-mouse-IgG monoclonal (Dianova GmbH) coupled to HRP was used as secondary antibody.

RESULTS

Tetracycline-controlled alternative splicing in HeLa cells

Based on the described engineered *hluc*+ gene cassette (15), tetracycline-responsive regulatory devices were generated to control exon skipping in HeLa cells. The coding frame of the *hluc*+ gene is split into two exons by insertion of an artificial intron-alternative exon-intron cassette (Figure 1). Each intron flanking the alternative exon has a 5′- and a 3′-SS. The used alternative exon harbors a PTC. Depending on the usage of the present SS, either the artificial exon is included into the coding region, yielding a transcript susceptible to NMD, or the alternative exon is skipped and the functional protein can be translated. This exon skipping process can be controlled by inserting the 5′-SS sequence of the second intron into the closing stem P1 of the tetracycline aptamer, thereby interfering with the accessibility of the SS and the subsequent spliceosome assembly process (29,30). In the ligand-unbound state, the aptamer is in a loose, open conformation and the 5′-SS is accessible (13,14). Binding of tetracycline then results in a more rigid conformation of the aptamer stem P1 and leads to masking of the 5′-SS. This prevents the alternative exon from being spliced into the coding sequence of the *hluc*+ gene. As a consequence, the functional protein can be expressed.

We inserted the tetracycline aptamer with the 5′-SS located upstream of the ligand-binding pocket (5′-SSup),

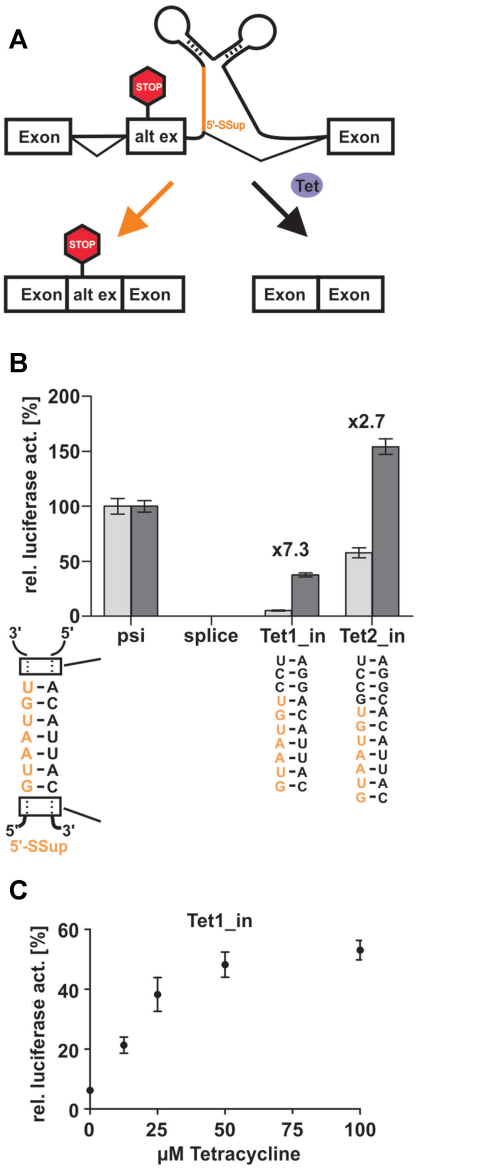

Figure 2. Tetracycline-induced exon skipping. (**A**) Schematic representation of tetracycline-induced exon skipping. The 5′-SS is placed into the closing stem of the tetracycline aptamer upstream of the ligand-binding pocket. In the absence of tetracycline, the alternative exon is included into the coding region of the gene of interest. The aptamer sequence remains part of the intron. In the presence of tetracycline (Tet, purple oval), the 5′-SS is masked, the alternative exon is skipped, and the functional protein is translated. (**B**) Luciferase activity measurement of splicing constructs. The ratios between the firefly and *Renilla* luciferase are shown relative to the respective control without (light-grey) or with (dark-gray) 50 μM tetracycline, which were set to 100%. Numbers above the bars indicate the dynamic range of regulation for each construct. Error bars represent the standard deviation of the mean values ($n = 3$). Corresponding sequences of the closing stem P1 are depicted underneath the graph. (**C**) Dose-dependent luciferase activity of the construct Tet1_in. SS, splice site; alt ex, alternative exon.

leaving the aptamer sequence as part of the intron (Figure 2). If the exon is skipped, the aptamer sequence is removed with the second intron, and only the alternative exon is spliced into the coding region. HeLa cells were transiently transfected with these constructs and incubated with or without 50 μM tetracycline for 24 h. Activity of the firefly luciferase (hluc+) was measured and normalized to the expression of the *Renilla* luciferase (*hRluc*), which is encoded on the same plasmid and serves as internal control. Relative luciferase expression was then calculated in relation to the parental, unmodified dual-luciferase vector (psi). This system allows for quantification of the dynamic range of the introduced switches on a protein level. First, a splicing control was measured that carries the engineered *hluc*+ intron-alternative exon-intron cassette without any interfering aptamer (Figure 2B). This 'splice' control shows no expression of intact firefly luciferase in the absence or presence of tetracycline and proves that very tight regulation with no background expression is possible upon inclusion of the alternative exon. The constructs Tet1_in and Tet2_in (as part of the intron) differ in their overall stem lengths and stability, with an additional GC base pair in the stem of Tet2_in (Figure 2B). Both constructs show exon skipping activity and an increase in luciferase activity in the presence of tetracycline. Tet1_in shows very low background expression, and luciferase activity can be induced up to 7.3-fold in a dose-dependent manner (Figure 2B and C). Tet2_in, on the other hand, shows strong background expression in the absence of tetracycline, suggesting that the more rigid closing stem of the aptamer disturbs recognition of the 5′-SS even in the non-ligand-bound aptamer conformation. To test whether the change in gene expression is in fact a consequence of tetracycline binding to its aptamer, a binding-deficient variant of Tet1_in (Tet1_inA9U) was tested in parallel, and no change in luciferase activity could be detected in the presence of tetracycline (Supplementary Figure S3).

Given that the intron sequences that were used have a GC content of only ∼35% and are therefore comparably unstructured, we hypothesized that highly structured RNA motives like the tetracycline aptamer might in general interfere with the splicing process due to steric hindrance (31). As we aimed for gene switches with a very tight off-state, we changed the system to enhance the level of alternative splicing events. We therefore placed the 5′-SS into the closing stem downstream of the aptamer-binding pocket (5′-SSdw), leaving the aptamer sequence as part of the exon instead of the intron (Figure 3). To maintain the stability of the aptamer stem, we first kept the connection sequences between the 5′-SS and the aptamer of Tet1_in and Tet2_in and placed the 5′-SS downstream of the communication modules to create the constructs Tet3_ex and Tet4_ex (as part of the exon). Tet3_ex shows an even lower background expression than Tet1_in and an increased dynamic range of the switch to 14.3-fold induction (Figure 3B and C). The Tet4_ex construct, however, lost its switching ability completely and the 5′-SS seems not to be addressed in either condition. We analyzed the generated sequences using the Human Splicing Finder 3.1 (32,33). Sequence analysis revealed the formation of an exonic splicing silencer (ESS: AGGC|Intron) that diminishes inclusion of the alternative exon (34,35). Further constructs (Tet5_ex-Tet9_ex) were then designed with an AG|GUAAUGU Exon|Intron intersection to avoid generating potent ESS elements (Figure 3B). The constructs Tet5_ex-Tet9_ex differ in terms of stem stability and the position of the 5′-SS within the closing stem. An overview of the stem characteristics is

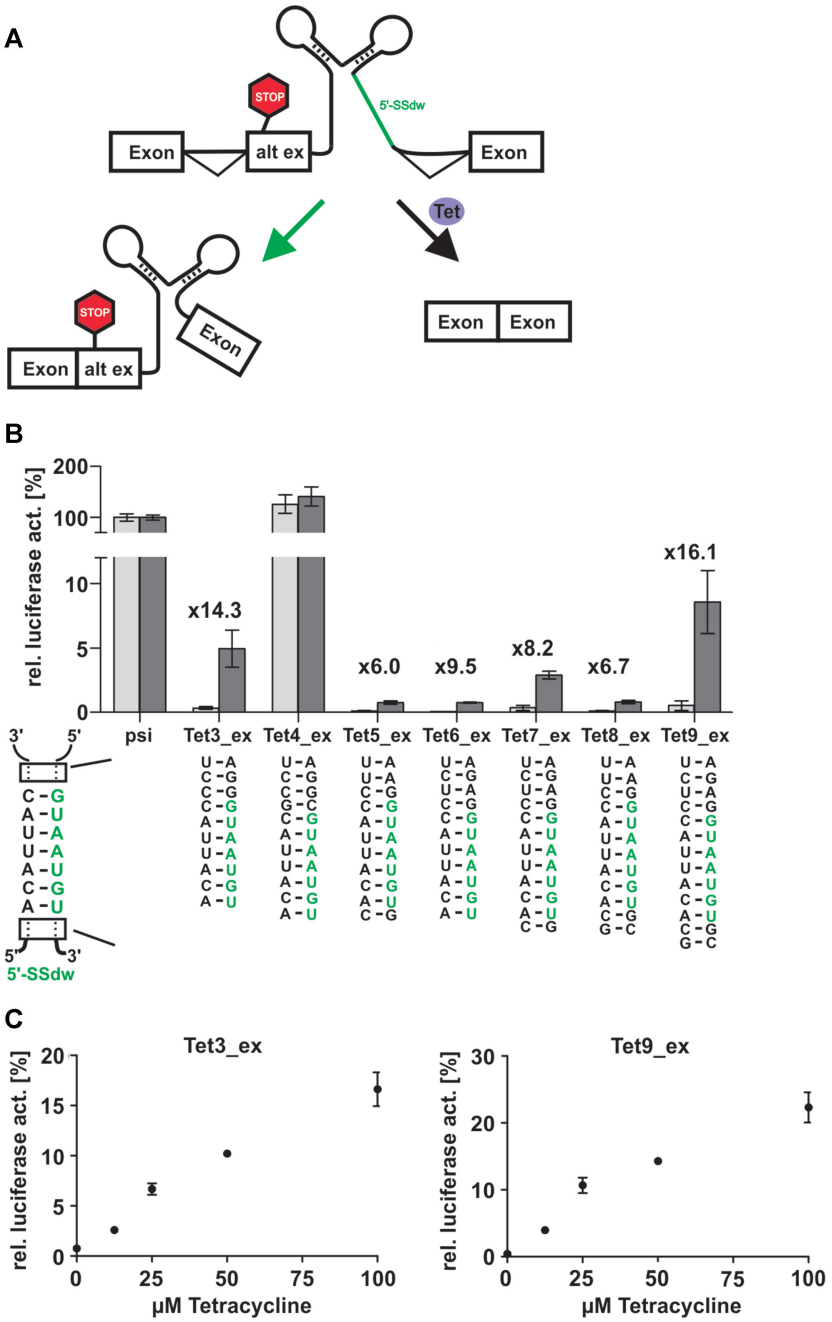

Figure 3. Tetracycline aptamer as part of the alternative exon. (**A**) Schematic representation of tetracycline-induced exon skipping. The 5′-SS is placed into the closing stem of the tetracycline aptamer downstream of the ligand-binding pocket. In the absence of tetracycline, the alternative exon is included into the coding region of the gene of interest. The aptamer sequence remains part of the exon. In the presence of tetracycline (Tet, purple oval), the 5′-SS is masked, the alternative exon is skipped, and the functional protein is translated. (**B**) Luciferase activity measurement of splicing constructs. The ratios between the firefly and *Renilla* luciferase are shown relative to the respective control without (light-grey) or with (dark-gray) 50 μM tetracycline, which were set to 100%. Numbers above the bars indicate the dynamic range of regulation for each construct. Error bars represent the standard deviation of the mean values ($n = 3$). Corresponding sequences of the closing stem P1 are depicted underneath the graph. (**C**) Dose-dependent luciferase activity of the constructs Tet3_ex and Tet9_ex. SS, splice site; alt ex, alternative exon.

given in Supplementary Figure S4. All constructs show very low background expression and exhibit robust tetracycline-dependent exon skipping. The strongest increase in reporter gene expression was achieved with construct Tet9_ex (16.1-fold). Dose-dependence tests indicate that even higher protein levels can be reached with increased tetracycline concentrations (100 μM) (Figure 3C). The data show that exon skipping can be achieved with the aptamer structure as part of the alternative exon sequence. This indicates a high flexibility concerning the sequence of the alternative exon that is used.

Controlling splicing without the need for additional exons

In order to further optimize the design, we aimed to keep the sequence inserted into the gene of interest as short as possible and envisioned that the aptamer alone, without an additional exon, should be sufficient to regulate gene expression. Placing the 5′-SS downstream of the aptamer-binding pocket and thus leaving the aptamer as part of the alternative exon opens the possibility of using the tetracycline aptamer not only for ligand-induced conformational change but also as an element that is able to fulfill the function of the alternative exon containing the PTC. Recognizing a stop codon (UAA) within the junction site of P1, P2 and P3 of the aptamer, we reasoned that the presence of the UAA trinucleotide should be sufficient to repress gene expression if it is placed in frame with the luciferase-encoding ORF. The stem lengths of the constructs Tet3_ex (9 nt) and Tet9_ex (12 nt) allow us to use the UAA in frame as a PTC and to remove the alternative exon sequence to create the splicing devices Tet10_el and Tet11_el (exon less). Full sequences of the aptamers are given in Supplementary Figure S5. The aptamer itself now embodies the alternative exon with an in-frame stop codon (Figure 4A and B).

Both constructs exhibit exon skipping activity in the presence of tetracycline (Figure 4C). Tet10_el shows a rather strong background expression and a 3-fold induction of luciferase activity that reaches close to 100% relative luciferase expression. Although Tet10_el displays one of the weakest performances of the designed switches regarding the dynamic range, it is nevertheless remarkable with regard to the absolute expression level in the presence of tetracycline. Such constructs could be of interest for applications where high protein levels are necessary to exert an effect and the considerably high background expression in the un-induced state is not of concern. The second construct, Tet11_el, is characterized by a more stable stem structure containing the 5′-SS. It shows reduced overall expression and an induction of 7.5-fold in the presence of tetracycline with a performance similar to Tet1_in. As already observed with Tet10_el, the Tet11_el construct likewise induces an overall higher expression level compared to Tet3_ex and Tet9_ex. Additionally, the switches Tet10_el and Tet11_el show a high responsiveness to lower tetracycline concentrations, reaching high protein expression levels already at 25 μM tetracycline (Figure 4D). Based on Tet11_el, we further fine-tuned the expression levels in the OFF- and ON-state. In construct Tet12_el, we decreased the distance between the aptamer-binding pocket and the splice site by 1 bp while maintaining the overall stability and stem lengths (Supplementary Figures S4 and 5). This approach results in an increased dynamic range of 12-fold and a higher expression level in the presence of tetracycline. In construct Tet13_el, we slightly destabilized the closing stem P1 of Tet11_el by changing the final GC to an AU base pair. This results in even less background expression and an induction level of 50% of the control expression with a dynamic range of 16.9-fold.

To verify that the presented changes in luciferase activity are a direct consequence of altered mRNA levels, RT-PCR was performed for the switches Tet1_in, Tet3_ex and Tet10_el. Following reverse transcription, PCR was performed with primers binding on exon1 and exon 2 of the split *hluc*+ coding frame (Figure 4D). Bands representing the functionally spliced mRNA are observed at 150 bp. The different constructs show bands for the functional mRNA with differences in intensity in the absence or presence of tetracycline. (The complete gel is shown in Supplementary Figure S6.) For quantification of relative *hluc*+ mRNA abundance, we chose primer pairs that bind to the coding sequence upstream of the splicing cassette for qPCR analysis (Figure 4E). The highest difference in mRNA levels can be observed in the constructs Tet1_in and Tet10_el, which show a 1.9-fold increase in *hluc*+ mRNA in the presence of tetracycline. qPCR data of the splice control shows a 2-fold decrease in mRNA levels compared to the psi positive control, while no band for functional mRNA could be detected via RT-PCR (Figure 4D and E). Since we would also detect unspliced und partially spliced RNA in this approach, we additionally performed qPCR with exon spanning primers to target only the mature mRNA. However, RNA levels were extremely low and hard to quantify. Subsequent analysis via agarose gel electrophoresis also discloses a side reaction and the product for alternatively spliced mRNA (Supplementary Figure S6). Nevertheless, all tested switches show a larger amount of functional mRNA in the presence of tetracycline.

The data on protein as well as on RNA level show that the tetracycline aptamer itself can be employed as an alternative exon for efficient splicing-based RNA switches. The approach requires only small sequence elements (∼60 bp) added to the coding region of the gene of interest for strong absolute gene expression levels to be achieved.

Tetracycline-induced exon skipping in *C. elegans*

We have shown previously that tetracycline is a suitable ligand for controlling gene expression via artificial riboswitches in *C. elegans* (21). With its low toxicity and good bioavailability, it was used to regulate transgene expression by controlling a tetracycline-dependent ribozyme that was inserted into the 3′-UTR of genes of interest. Although the system proved to be robust and convenient and allowed us to control expression in a tissue-specific manner, its drawback was the rather low dynamic range of maximal 3.8-fold induction upon tetracycline addition. Since the developed splicing switches in the above-described experiments in human cell culture performed significantly better compared to tetracycline-dependent aptazymes, we transferred them to the nematode *C. elegans*. The splicing constructs Tet1_in, Tet3_ex and Tet10_el each present different varia-

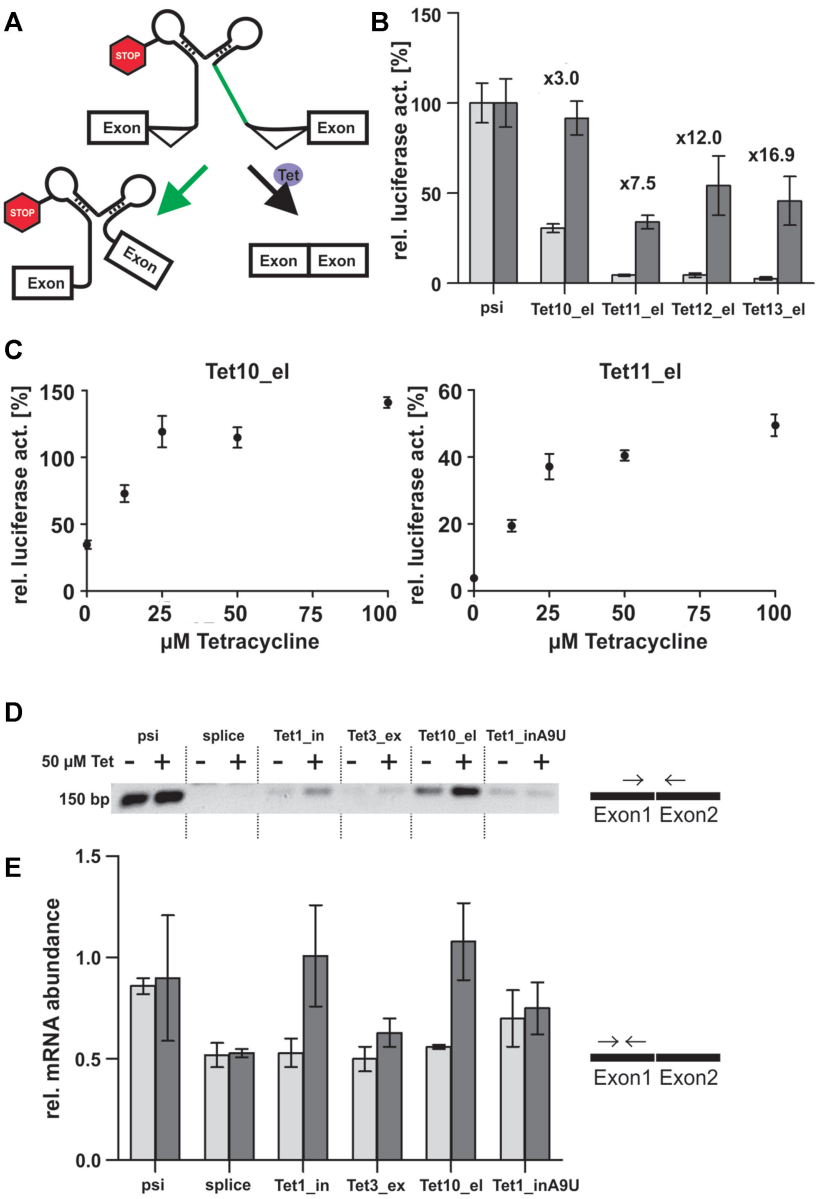

Figure 4. Tetracycline aptamer as alternative exon. (**A**) Schematic representation of tetracycline-induced exon skipping with the aptamer sequence harboring an in-frame stop codon (red hexagon). In the absence of tetracycline, the aptamer sequence is spliced into the coding region, whereas in its presence, the 5′-SS is masked and the functional protein is translated. (**B**) Luciferase activity measurement of the respective constructs. The ratios between the firefly and *Renilla* luciferase are shown relative to the respective control without (light-grey) or with (dark-gray) 50 μM tetracycline, which were set to 100%. Numbers above the bars indicate the dynamic range of regulation for each construct. Error bars represent the standard deviation of the mean values ($n = 3$). (**C**) Dose-dependent luciferase activity of the constructs Tet10_el and Tet11_el. (**D**) HeLa cells were transiently transfected with the indicated constructs and cultivated in the presence or absence of 50 μM tetracycline for 24 h. Total RNA was prepared and used for RT-PCR with primer pairs binding to both exons of *hluc*+. psi: original vector w/o splicing cassette, splice: control construct with the splicing cassette but without aptamer, Tet1_inA9U harbors a point mutation at position 9 of the aptamer, rendering the aptamer binding deficient. The band at 150 bp, which resembles the functional *hluc*+ mRNA, is shown. (**E**) Relative *hluc*+ mRNA abundance was determined via qPCR for RNA isolated in (D) with primers that bind exclusively to exon1. *hluc*+ mRNA levels were normalized to *hRluc* values. Error bars represent the standard deviation of the mean values ($n = 3$).

tions of our design and show great differences in their dynamic ranges and the overall expression levels. They were therefore considered to be promising candidates for induction of gene expression in *C. elegans*. In general, *C. elegans* possesses an intron-rich genome. These introns differ greatly in size from human introns: 56% of *C. elegans* introns are smaller than 100 nt (36). We implemented our system into a ubiquitously expressed mCherry reporter gene driven by the *icd-2* promotor (21). The reporter gene consists of 4 exons and 3 synthetic introns, each having a length of 51 nt (Supplementary Figure S7). The splicing constructs Tet1_in and Tet3_ex, containing the alternative exon, and Tet10_el, harboring the PTC within the aptamer sequence, were placed downstream of the first mCherry intron. An additional intron of 51 nt was inserted downstream of the aptamer to create the respective splicing systems CeTet1_in,

CeTet3_ex and CeTet10_el, which are analogous to their counterparts in human cell culture experiments (Figure 5). Transgenic strains were generated carrying the different mCherry constructs along with a ubiquitously expressed GFP co-marker driven by the dpy-30 promotor. To rule out unspecific effects of tetracycline on our reporter, animals constitutively expressing mCherry served as control. An additional 'splice' control consisting of the alternative exon and the additional intron was used, but its 5′-SS was not masked by an aptamer (analogous to the 'splice' control in HeLa cells). This construct shows no detectable expression in the presence or absence of tetracycline, thus demonstrating the tight control that is possible with our system (Supplementary Figure S8). After the incubation of transgenic worms with or without 10 μM tetracycline for 3 days from hatch until adulthood, 5 respective animals were picked and the mCherry expression was monitored by fluorescence microscopy (Figure 5A). CeTet1_in, carrying the 5′-SS upstream of the tetracycline-binding pocket, shows no difference in mCherry expression compared to the control animals, suggesting the alternative exon is always skipped and gene expression can occur. In contrast, CeTet3_ex and CeTet10_el show strong expression in the presence of tetracycline, while no mCherry expression is visible in the absence of tetracycline. The aptamer sequence as part of the alternative exon instead of the intron seems to favor alternative splicing events in *C. elegans*, and immunoblot analysis confirmed the regulatory effect of the inserted constructs on mCherry expression (Figure 5B). CeTet3_ex shows strong induction of mCherry expression, while no background expression is detectable. A dilution series of samples drawn from a *C. elegans* culture carrying CeTet3_ex demonstrates an over 20-fold induction of mCherry expression in comparison to the uninduced culture (Supplementary Figure S9).

Given the very tight and efficient gene regulation with the developed CeTet3_ex switch, this construct was subsequently applied to generate a conditional *C. elegans* model of human Huntington's disease. This disease is caused by the expression of the polyglutamine-expanded protein Huntingtin (Htt), which is highly aggregation-prone and neurotoxic above a threshold of 35 glutamines (35Q) (37,38). Using the CeTet3_ex switch, we generated transgenic *C. elegans* strains that express an Htt-GFP construct containing a pathogenic, aggregation-prone stretch of 103Q (Htt103Q::GFP). In addition, we constructed control strains expressing Htt-GFP with a non-pathogenic soluble polyQ repeat of 25Q (Htt25Q::GFP) (Figure 5C). While both the Htt25Q and Htt103Q::GFP fusion protein are strongly induced upon tetracycline application, only the 103Q version shows protein aggregate formation, while the 25Q version remains soluble (Figure 5C). RT-PCR analysis confirms the formation of functional mRNA only in the presence of tetracycline, and follow-up qPCR analysis confirms increased mRNA levels (Supplementary Figure S11). Thus, the CeTet3_ex switch allows for ubiquitous induction and *in vivo* investigation of highly toxic protein variants that would be lethal or cause severe developmental defects in constitutive expression models. These data demonstrate that the artificial riboswitch CeTet3_ex is a valuable genetic tool for inducible gene expression in the widely used model organism *C. elegans*.

DISCUSSION

Engineered systems for conditional control of transgene expression are very important tools for studying cellular functions, and they hold great promise for controlling transgene expression in future therapeutic applications. In many cases, synthetic genetic control elements rely on the use of conditional promotors and regulatory proteins that often show leaky basal expression and high species specificities (39). These control elements do create the necessity of introducing additional regulatory proteins that need to be expressed at defined levels in order to exert the desired control (39). Moreover, they pose the risk of immunogenic reactions to the protein factors that are used. The use of artificial riboswitches to regulate gene expression on an RNA level overcomes these limitations of transcription factor-based systems. The direct interaction of RNA with a small-molecule ligand allows for tissue-specific gene regulation with greatly reduced off-target effects in a variety of systems (40). However, the construction of potent synthetic riboswitches in mammalian systems is still challenging. While the development of artificial riboswitches in bacteria or yeast can be achieved via effective and low-cost screening approaches, these riboswitches proved in many cases to be untransferable to human cell systems (5,9,41,42). In order to efficiently identify riboswitches, which are functional *in vivo*, we have recently introduced an NGS-based screening method that allows for sampling diverse libraries of potential riboswitches (11). However, the development of robust RNA-based systems for controlling gene expression that can be optimized easily based on rational designs and testing of relatively few sequence variants is of high importance. In this regard, the introduced system that relies on aptamer-based control of alternative splicing represents a significant step toward the goal of developing universally applicable, efficient, and robust genetic switches of gene expression.

Given the broad distribution of alternative splicing across many eukaryotic species, we created artificial riboswitches based on an exon skipping mechanism for conditional control of gene expression in HeLa cells and the model organism *C. elegans*. The tetracycline aptamer was chosen as the sensory domain since it has already been successfully coupled to various expression platforms and has been shown to exhibit gene regulatory activity in many organisms, including the nematode *C. elegans* (8,10,21,25). The conformational change within the aptamer upon tetracycline binding leads to a stabilized structure of the closing stem P1, which is not important for ligand recognition. This opens opportunities to control the function of sequences embedded in this P1 stem (14,43,44).

In the presented work, we have focused on the sequestration of the 5′-SS of an engineered intron-alternative exon-intron system to control its accessibility for important splicing factors. The 5′-SS of the second intron is included into the closing stem P1 of the tetracycline aptamer. In its loose, ligand-unbound state, the SS is accessible and the alternative exon, which harbors a PTC, is included into the coding sequence and represses functional protein expression (16,17). In the presence of tetracycline, the 5′-SS is masked, the alternative exon is skipped, and the functional, full-length protein is translated. Varying the stability of stem P1

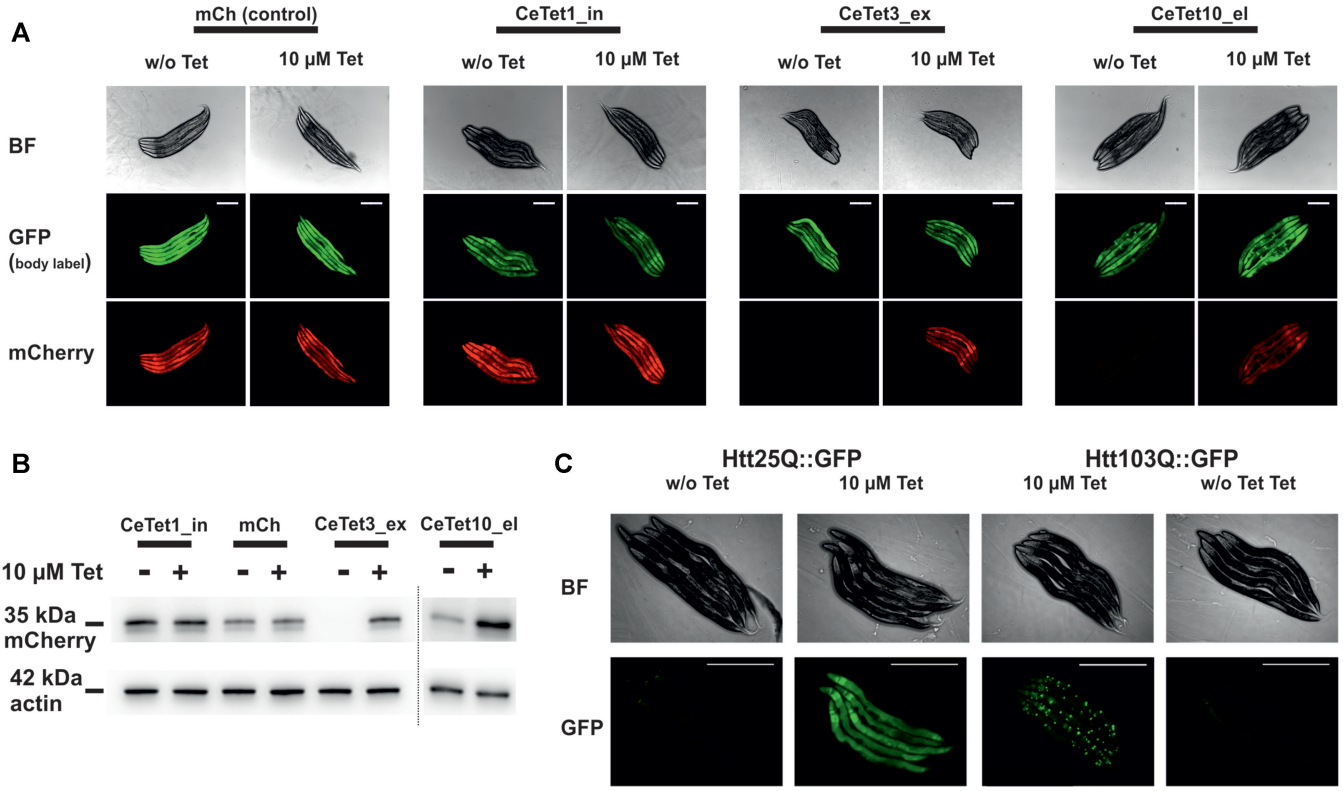

Figure 5. Tetracycline mediated gene expression in *C. elegans*. (**A**) Fluorescent images of transgenic worms carrying different splicing constructs. For each construct a stack of 5 worms is shown. Animals were grown in the absence or presence of tetracycline for 3 days from hatch until adulthood. Transgenic animals were chosen using the GFP body label. Scale bar represents 200 µm. (**B**) Western blot analysis of mCherry expression is shown in worms carrying different splicing constructs grown in the absence and presence of 10 µM tetracycline. (**C**) Fluorescent microscope images of worms expressing Huntingtin-GFP harboring stretches of 25 glutamines (Htt25Q::GFP) or 103 glutamines (Htt103Q::GFP). Animals were grown in the presence or absence of 10 µM tetracycline for 3 days from hatch until adulthood. Scale bar represents 500 µm. Tet, tetracycline; BF, bright field; mCh, mCherry

allows for fine-tuning of expression levels by rational design. We present data showing that the position of the aptamer within the splicing constructs influences basal and induced gene expression levels. The aptamer sequence as part of the intron as seen in constructs Tet1_in and Tet2_in leads to higher expression levels than in the constructs Tet3_ex-Tet9_ex, where the aptamer is part of the alternative exon spliced into the coding region. The removal of the alternative exon and usage of an in-frame stop codon within the aptamer (constructs Tet10_el and Tet11_el) increases protein expression in comparison to the constructs carrying the alternative exon. Variations of the closing stem P1 thereby allow fine-tuning of the basal and induced expression levels as seen in constructs Tet12_el and Tet13_el. The designed constructs that exhibit exon skipping activity differ greatly in terms of their dynamic range (2.7–16.9-fold) and the protein expression level. This broadens the range of applications for such switches since it opens up the possibility of using variations of the system regarding different needs of absolute protein levels. In addition, we demonstrate the straightforward transfer of the system to the multicellular organism *C. elegans* with a strong induction of protein expression in the presence of 10 µM tetracycline. *C. elegans* is a widely used model organism for which convenient inducible gene expression systems with a high dynamic range are scarce. As previously shown with ribozyme-based RNA switches, using tetracycline as ligand allows for induction in all somatic tissues of the *C. elegans* worm, including muscles and neurons (21). The presented exon skipping constructs of this study show superior performance even compared to these ribozyme constructs. Given the high dynamic range (>20-fold; see Supplementary Figure S9), the CeTet3_ex switch represents a valuable new genetic tool for conditional gene expression in *C. elegans*. The applicability of this system in *C. elegans* is demonstrated by the robust tetracycline-dependent induction of the metastable and aggregation-prone Htt103Q::GFP, which forms Htt inclusions throughout the body of the worm. Considering the relatively small genetic modification necessary for introducing the CeTet3_ex switch and the possibility of applying it to any gene of interest with retaining natural promoters as well as 5′- and 3′-UTRs, this tool should be broadly applicable in *C. elegans*.

Taken together, we present RNA-based gene regulatory devices that function robustly and efficiently in two distantly related eukaryotic species. Given their size, the presented constructs leave a small genetic footprint, are easy to apply, and use a ligand that could also be applied in future therapeutic strategies in humans. This approach can therefore be adapted to a variety of applications. A recent application of tetracycline-dependent aptazymes in mice demonstrated efficient (up to 15-fold) induction of gene expression

with 100 mg/kg administered tetracycline (45–47). In addition, since the transfer of our system from human cells to *C. elegans* was successful, we anticipate that the application of the presented RNA switches in further animal models should be feasible.

DATA AVAILABILITY

Data and materials are available upon request.

SUPPLEMENTARY DATA

Supplementary Data are available at NAR Online.

ACKNOWLEDGEMENTS

We are grateful for materials provided by the lab of Prof. Dr Elke Deuerling (University of Konstanz) and would like to thank Astrid Joachimi and Renate Schlömer for technical assistance.

FUNDING

Deutsche Forschungsgemeinschaft (DFG) within the collaborative research center SFB 969 'Chemical and Biological Principles of Cellular Proteostasis' [TP A05 to J.S.H., TP A07 to M.G.]. Funding for open access charge: Deutsche Forschungsgemeinschaft (DFG) within the collaborative research center SFB 969 'Chemical and Biological Principles of Cellular Proteostasis'.
Conflict of interest statement. None declared.

REFERENCES

1. Gossen,M., Freundlieb,S., Bender,G., Muller,G., Hillen,W. and Bujard,H. (1995) Transcriptional activation by tetracyclines in mammalian cells. *Science*, **268**, 1766–1769.
2. Berens,C. and Hillen,W. (2003) Gene regulation by tetracyclines. Constraints of resistance regulation in bacteria shape TetR for application in eukaryotes. *Eur. J. Biochem.*, **270**, 3109–3121.
3. Wei,X., Potter,C.J., Luo,L. and Shen,K. (2012) Controlling gene expression with the Q repressible binary expression system in *Caenorhabditis elegans*. *Nat. Methods*, **9**, 391–395.
4. Roth,A. and Breaker,R.R. (2009) The structural and functional diversity of metabolite-binding riboswitches. *Annu. Rev. Biochem.*, **78**, 305–334.
5. Berens,C., Groher,F. and Suess,B. (2015) RNA aptamers as genetic control devices: the potential of riboswitches as synthetic elements for regulating gene expression. *Biotechnol. J.*, **10**, 246–257.
6. Werstuck,G. and Green,M.R. (1998) Controlling gene expression in living cells through small molecule-RNA interactions. *Science*, **282**, 296–298.
7. Liu,Y., Li,J., Chen,Z., Huang,W. and Cai,Z. (2018) Synthesizing artificial devices that redirect cellular information at will. *Elife*, **7**, e31936.
8. Mou,H., Zhong,G., Gardner,M.R., Wang,H., Wang,Y.W., Cheng,D. and Farzan,M. (2018) Conditional regulation of gene expression by ligand-induced occlusion of a microRNA target sequence. *Mol. Ther.*, **26**, 1277–1286.
9. Sack,M., Stifel,J., Kreft,S.G., Deuerling,E. and Hartig,J.S. (2019) Neomycin-dependent hammerhead ribozymes for the direct control of gene expression in Saccharomyces cerevisiae. *Methods*, **161**, 35–40.
10. Beilstein,K., Wittmann,A., Grez,M. and Suess,B. (2015) Conditional control of mammalian gene expression by tetracycline-dependent hammerhead ribozymes. *ACS Synth. Biol.*, **4**, 526–534.
11. Strobel,B., Sporing,M., Klein,H., Blazevic,D., Rust,W., Sayols,S., Hartig,J.S. and Kreuz,S. (2020) High-throughput identification of synthetic riboswitches by barcode-free amplicon-sequencing in human cells. *Nat. Commun.*, **11**, 714.
12. Wang,E.T., Sandberg,R., Luo,S., Khrebtukova,I., Zhang,L., Mayr,C., Kingsmore,S.F., Schroth,G.P. and Burge,C.B. (2008) Alternative isoform regulation in human tissue transcriptomes. *Nature*, **456**, 470–476.
13. Weigand,J.E. and Suess,B. (2007) Tetracycline aptamer-controlled regulation of pre-mRNA splicing in yeast. *Nucleic Acids Res.*, **35**, 4179–4185.
14. Vogel,M., Weigand,J.E., Kluge,B., Grez,M. and Suess,B. (2018) A small, portable RNA device for the control of exon skipping in mammalian cells. *Nucleic Acids Res.*, **46**, e48.
15. Boyne,A.R., Danos,F., Olivier, Volles,J., Michael and Guo,X. (2016) WO/2016/126747.
16. Nagy,E. and Maquat,L.E. (1998) A rule for termination-codon position within intron-containing genes: when nonsense affects RNA abundance. *Trends Biochem. Sci.*, **23**, 198–199.
17. Lewis,B.P., Green,R.E. and Brenner,S.E. (2003) Evidence for the widespread coupling of alternative splicing and nonsense-mediated mRNA decay in humans. *Proc. Natl. Acad. Sci. U.S.A.*, **100**, 189–192.
18. Berens,C., Thain,A. and Schroeder,R. (2001) A tetracycline-binding RNA aptamer. *Bioorg. Med. Chem.*, **9**, 2549–2556.
19. Argast,M. and Beck,C.F. (1984) Tetracycline diffusion through phospholipid bilayers and binding to phospholipids. *Antimicrob. Agents Chemother.*, **26**, 263–265.
20. Grossman,T.H. (2016) Tetracycline antibiotics and resistance. *Cold Spring Harb. Perspect. Med.*, **6**, a025387.
21. Wurmthaler,L.A., Sack,M., Gense,K., Hartig,J.S. and Gamerdinger,M. (2019) A tetracycline-dependent ribozyme switch allows conditional induction of gene expression in *Caenorhabditis elegans*. *Nat. Commun.*, **10**, 491.
22. Muller,M., Weigand,J.E., Weichenrieder,O. and Suess,B. (2006) Thermodynamic characterization of an engineered tetracycline-binding riboswitch. *Nucleic Acids Res.*, **34**, 2607–2617.
23. Xiao,H., Edwards,T.E. and Ferre-D'Amare,A.R. (2008) Structural basis for specific, high-affinity tetracycline binding by an in vitro evolved aptamer and artificial riboswitch. *Chem. Biol.*, **15**, 1125–1137.
24. Liu,Y., Zhan,Y., Chen,Z., He,A., Li,J., Wu,H., Liu,L., Zhuang,C., Lin,J., Guo,X. *et al.* (2016) Directing cellular information flow via CRISPR signal conductors. *Nat. Methods*, **13**, 938–944.
25. Suess,B., Hanson,S., Berens,C., Fink,B., Schroeder,R. and Hillen,W. (2003) Conditional gene expression by controlling translation with tetracycline-binding aptamers. *Nucleic Acids Res.*, **31**, 1853–1858.
26. Brenner,S. (1974) The genetics of *Caenorhabditis elegans*. *Genetics*, **77**, 71–94.
27. Mello,C. and Fire,A. (1995) DNA transformation. *Methods Cell Biol.*, **48**, 451–482.
28. Schindelin,J., Arganda-Carreras,I., Frise,E., Kaynig,V., Longair,M., Pietzsch,T., Preibisch,S., Rueden,C., Saalfeld,S., Schmid,B. *et al.* (2012) Fiji: an open-source platform for biological-image analysis. *Nat. Methods*, **9**, 676–682.
29. Rosbash,M. and Seraphin,B. (1991) Who's on first? The U1 snRNP-5′ splice site interaction and splicing. *Trends Biochem. Sci.*, **16**, 187–190.
30. Pomeranz Krummel,D.A., Oubridge,C., Leung,A.K., Li,J. and Nagai,K. (2009) Crystal structure of human spliceosomal U1 snRNP at 5.5 A resolution. *Nature*, **458**, 475–480.
31. Buratti,E. and Baralle,F.E. (2004) Influence of RNA secondary structure on the pre-mRNA splicing process. *Mol. Cell. Biol.*, **24**, 10505–10514.
32. 2013/2020 © Human Splicing Finder - Bioinformatics & Genetics Team - Inserm UMR 1251 - Aix Marseille Université, B.J.M., 13385 Marseille Cedex 05
33. Desmet,F.O., Hamroun,D., Lalande,M., Collod-Beroud,G., Claustres,M. and Beroud,C. (2009) Human splicing finder: an online bioinformatics tool to predict splicing signals. *Nucleic Acids Res.*, **37**, e67.
34. Sironi,M., Menozzi,G., Riva,L., Cagliani,R., Comi,G.P., Bresolin,N., Giorda,R. and Pozzoli,U. (2004) Silencer elements as possible inhibitors of pseudoexon splicing. *Nucleic Acids Res.*, **32**, 1783–1791.
35. Pozzoli,U. and Sironi,M. (2005) Silencers regulate both constitutive and alternative splicing events in mammals. *Cell. Mol. Life Sci.*, **62**, 1579–1604.

36. Zahler,A.M. (2012) Pre-mRNA splicing and its regulation in *Caenorhabditis elegans*. *WormBook*, 1–21.
37. Brignull,H.R., Moore,F.E., Tang,S.J. and Morimoto,R.I. (2006) Polyglutamine proteins at the pathogenic threshold display neuron-specific aggregation in a pan-neuronal Caenorhabditis elegans model. *J. Neurosci.*, **26**, 7597–7606.
38. Lee,A.L., Ung,H.M., Sands,L.P. and Kikis,E.A. (2017) A new *Caenorhabditis elegans* model of human huntingtin 513 aggregation and toxicity in body wall muscles. *PLoS One*, **12**, e0173644.
39. Mathur,M., Xiang,J.S. and Smolke,C.D. (2017) Mammalian synthetic biology for studying the cell. *J. Cell Biol.*, **216**, 73–82.
40. Sporing,M., Finke,M. and Hartig,J.S. (2019) Aptamers in RNA-based switches of gene expression. *Curr. Opin. Biotechnol.*, **63**, 34–40.
41. Stifel,J., Spöring,M. and Hartig,J.S. (2019) Expanding the toolbox of synthetic riboswitches with guanine-dependent aptazymes. *Synth. Biol.*, **4**, ysy022.
42. Townshend,B., Kennedy,A.B., Xiang,J.S. and Smolke,C.D. (2015) High-throughput cellular RNA device engineering. *Nat. Methods*, **12**, 989–994.
43. Demolli,S., Geist,M.M., Weigand,J.E., Matschiavelli,N., Suess,B. and Rother,M. (2014) Development of beta-lactamase as a tool for monitoring conditional gene expression by a tetracycline-riboswitch in *Methanosarcina acetivorans*. *Archaea*, **2014**, 725610.
44. Sporing,M., Boneberg,R. and Hartig,J.S. (2020) Aptamer-mediated control of polyadenylation for gene expression regulation in mammalian cells. *ACS Synth Biol*, **9**, 3008–3018.
45. Zhong,G., Wang,H., Bailey,C.C., Gao,G. and Farzan,M. (2016) Rational design of aptazyme riboswitches for efficient control of gene expression in mammalian cells. *Elife*, **5**, e18858.
46. Reid,C.A., Nettesheim,E.R., Connor,T.B. and Lipinski,D.M. (2018) Development of an inducible anti-VEGF rAAV gene therapy strategy for the treatment of wet AMD. *Sci. Rep.*, **8**, 11763.
47. Strobel,B., Duchs,M.J., Blazevic,D., Rechtsteiner,P., Braun,C., Baum-Kroker,K.S., Schmid,B., Ciossek,T., Gottschling,D., Hartig,J.S. *et al.* (2020) A small-molecule-responsive riboswitch enables conditional induction of viral vector-mediated gene expression in mice. *ACS Synth Biol*, **9**, 1292–1305.